Robotics 2

Final test in classroom – May 29, 2017

Exercise 1

Let the dynamics of a robot manipulator with n joints be described by the usual Lagrangian model (neglecting dissipative terms):

$$\boldsymbol{M}(\boldsymbol{q})\ddot{\boldsymbol{q}} + \boldsymbol{c}(\boldsymbol{q}, \dot{\boldsymbol{q}}) + \boldsymbol{g}(\boldsymbol{q}) = \boldsymbol{\tau}. \tag{1}$$

- List all feedback control laws for $\boldsymbol{\tau}$ that allow regulation to a desired (generic) constant configuration $\boldsymbol{q}_d$. For each control law, specify the design conditions that guarantee success, the type of convergence/stability achieved, and the pros and cons of the method.
- When applied to eq. (1), is it possible that the control law

$$\boldsymbol{\tau} = \boldsymbol{K}_P(\boldsymbol{q}_d - \boldsymbol{q}) - \boldsymbol{K}_D\dot{\boldsymbol{q}} \tag{2}$$

achieves asymptotic stabilization of a desired state $(\boldsymbol{q}, \dot{\boldsymbol{q}}) = (\boldsymbol{q}_d, \boldsymbol{0})$? If so, under which operative conditions? Would these conditions be only sufficient or also necessary?

- Can it happen that the following control law applied to eq. (1)

$$\boldsymbol{\tau} = \boldsymbol{g}(\boldsymbol{q}_d) + \boldsymbol{K}_P(\boldsymbol{q}_d - \boldsymbol{q}) - \boldsymbol{K}_D\dot{\boldsymbol{q}} \tag{3}$$

does *not* achieve asymptotic stabilization of the state $(\boldsymbol{q}, \dot{\boldsymbol{q}}) = (\boldsymbol{q}_d, \boldsymbol{0})$? Why (or why not)? What should be done in (3) to validate the reverse statement "does *certainly* achieve ..."?

Exercise 2

- In the context of image-based visual servoing (IBVS), determine the interaction matrix $\boldsymbol{J}_{p,polar}$ associated to a point feature $\boldsymbol{s} = (\rho \;\; \theta)^T \in \mathbb{R}^2$ which is parametrized with polar coordinates in the image plane, i.e.,

$$\dot{\boldsymbol{s}} = \begin{pmatrix} \dot{\rho} \\ \dot{\theta} \end{pmatrix} = \boldsymbol{J}_{p,polar}(\rho, \theta, \lambda, Z) \begin{pmatrix} \boldsymbol{V} \\ \boldsymbol{\Omega} \end{pmatrix},$$

where $\lambda > 0$ is the focal length of the camera, $Z > 0$ is the depth coordinate of the Cartesian point $P = (X, Y, Z)$ in the camera frame, and the perspective equations of a pinhole camera model are used.

- Discuss the characteristics of the obtained interaction matrix in terms of decoupled effects on the chosen feature parameters, when only single components of the linear velocity $\boldsymbol{V} \in \mathbb{R}^3$ or of the angular velocity $\boldsymbol{\Omega} \in \mathbb{R}^3$ are active. Compare this analysis with the one on the interaction matrix $\boldsymbol{J}_p$ that uses the Cartesian coordinates (u, v) in the image plane.
- In an IBVS control law that regulates the polar coordinates of a point feature $\boldsymbol{s}$ to a desired constant value $\boldsymbol{s}_d$, what careful actions may be needed when the point P is on or gets close to the optical axis of the camera?

Exercise 3

Consider the planar PRP robot in Fig. 1, moving under gravity. Its dynamic model can be written in the form

$$\boldsymbol{Y_M}(\boldsymbol{q}, \dot{\boldsymbol{q}}, \ddot{\boldsymbol{q}})\, \boldsymbol{a_M} + \boldsymbol{g}(\boldsymbol{q}) = \boldsymbol{\tau}, \tag{4}$$

where the inertial terms and the related Coriolis and centrifugal components are already expressed in a linear factorized form in terms of the dynamic coefficients $\boldsymbol{a_M} \in \mathbb{R}^{p_M}$. In the following, assume that the symbolic expressions of $\boldsymbol{Y_M}$ and $\boldsymbol{a_M}$ are known.

- Derive explicitly the gravity term $\boldsymbol{g}(\boldsymbol{q})$ and an associated minimal factorization in the form $\boldsymbol{g}(\boldsymbol{q}) = \boldsymbol{Y_g}(\boldsymbol{q})\, \boldsymbol{a_g}$, with $\boldsymbol{a_g} \in \mathbb{R}^{p_g}$.
- Provide the expression of an adaptive control law that guarantees global asymptotic tracking of a desired joint trajectory $\boldsymbol{q}_d(t) \in C^2$, without any a priori knowledge of the numerical values of the robot dynamic parameters. How many states will have this dynamical controller?
- Assume now that the actual values of the dynamic coefficients $\boldsymbol{a_M}$ are known in advance. Solve the previously stated trajectory tracking problem by designing an adaptive controller that has a reduced number of states. Sketch a formal proof of your result.

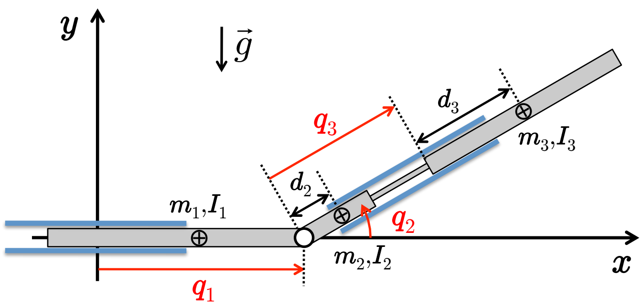

Figure 1: A planar PRP robot, with an associated set of generalized coordinates $\boldsymbol{q} = (q_1, q_2, q_3)$.

Figure 2: Robotized surface polishing of a metallic work piece.

Exercise 4

Consider a robotized polishing task of a large surface area of a metallic work piece, as shown in Fig. 2. The work piece has a complex geometry, with planar and curved surfaces. The polishing tool held by the robot ends with a sphere which is in point-wise contact with the geometric surface of the work piece. The tool needs not to be orthogonal to the local tangent plane to the surface. However, in order to complete an optimal polishing (reducing the roughness of the surface below a specified level —with tolerances in the order of few μm), a specified normal force should be applied to the surface while moving the tool in contact with an assigned constant speed. Assume a perfectly rigid interaction and that friction at the contact can be neglected in this modeling stage.

Define a task frame in which the polishing operation can be correctly defined and executed. Specify accordingly the natural and artificial constraints. Sketch the task frame in two cases, on a flat surface of the work piece and on a curved one.

[240 minutes (4 hours); open books, but no computer or smartphone]

Solution

May 29, 2017

Exercise 1

The first part is a free text exercise. Completeness, accuracy, and clarity in writing are evaluated.

For the two other specific questions:

- The control law (2) achieves asymptotic stabilization of a desired state $(\boldsymbol{q}, \dot{\boldsymbol{q}}) = (\boldsymbol{q}_d, \boldsymbol{0})$ also in the presence of gravity if: *i)* $\boldsymbol{g}(\boldsymbol{q}_d) = \boldsymbol{0}$ (the desired configuration is an unforced equilibrium for the open-loop system); *ii)* $\boldsymbol{K}_P$ is symmetric and positive definite, and its minimum eigenvalue $\boldsymbol{K}_{P,m} > \alpha$, where $\alpha > 0$ is a global upper bound on the norm of the Hessian of the potential energy $U_g(\boldsymbol{q})$ due to gravity; *iii)* $\boldsymbol{K}_D$ is symmetric and positive definite. In general, these are only sufficient conditions.

- Even assuming that $\boldsymbol{K}_P$ and $\boldsymbol{K}_D$ are symmetric and positive definite, the control law (3) may still fail because $\boldsymbol{K}_{P,m} \leq \alpha$. Indeed, when this sufficient condition is violated, we cannot predict if we will obtain asymptotic stabilization of the desired equilibrium state or not.

Exercise 2

Using the pinhole model, a 3D Cartesian point $\boldsymbol{P} = (X, Y, Z)$, with coordinates expressed in the camera frame, becomes in the image plane a point feature (u, v)

$$u = \lambda \frac{X}{Z}, \qquad v = \lambda \frac{Y}{Z},$$

when 2D Cartesian coordinates are used, being $\lambda > 0$ the focus length of the camera. These two feature parameters move in the image plane in response to a linear and angular velocity of the camera, respectively $\boldsymbol{V}$ and $\boldsymbol{\Omega}$, as

$$\begin{pmatrix} \dot{u} \\ \dot{v} \end{pmatrix} = \begin{pmatrix} \frac{\lambda}{Z} & 0 & -\frac{u}{Z} \\ 0 & \frac{\lambda}{Z} & -\frac{v}{Z} \end{pmatrix} \begin{pmatrix} \dot{X} \\ \dot{Y} \\ \dot{Z} \end{pmatrix},$$

$$\begin{pmatrix} \dot{X} \\ \dot{Y} \\ \dot{Z} \end{pmatrix} = -\boldsymbol{V} - \boldsymbol{\Omega} \times \boldsymbol{P} = \begin{pmatrix} -1 & 0 & 0 & 0 & -Z & Y \\ 0 & -1 & 0 & Z & 0 & -X \\ 0 & 0 & -1 & -Y & X & 0 \end{pmatrix} \begin{pmatrix} \boldsymbol{V} \\ \boldsymbol{\Omega} \end{pmatrix}$$

$$\Rightarrow \quad \begin{pmatrix} \dot{u} \\ \dot{v} \end{pmatrix} = \begin{pmatrix} -\frac{\lambda}{Z} & 0 & \frac{u}{Z} & \frac{uv}{\lambda} & -\left(\lambda + \frac{u^2}{\lambda}\right) & v \\ 0 & -\frac{\lambda}{Z} & \frac{v}{Z} & \lambda + \frac{v^2}{\lambda} & -\frac{uv}{\lambda} & -u \end{pmatrix} \begin{pmatrix} \boldsymbol{V} \\ \boldsymbol{\Omega} \end{pmatrix} = \boldsymbol{J}_p(u, v, \lambda, Z) \begin{pmatrix} \boldsymbol{V} \\ \boldsymbol{\Omega} \end{pmatrix}.$$

When using instead the polar coordinates as feature parameters in the image plane, we have the transformations

$$\begin{pmatrix} u \\ v \end{pmatrix} = \begin{pmatrix} \rho \cos\theta \\ \rho \sin\theta \end{pmatrix} \qquad \Longleftrightarrow \qquad \begin{pmatrix} \rho \\ \theta \end{pmatrix} = \begin{pmatrix} \sqrt{u^2 + v^2} \\ \mathrm{ATAN2}\{v, u\} \end{pmatrix}$$

$$\Rightarrow \quad \begin{pmatrix} \dot{u} \\ \dot{v} \end{pmatrix} = \begin{pmatrix} \dot{\rho} \cos\theta - \rho\dot{\theta} \sin\theta \\ \dot{\rho} \sin\theta + \rho\dot{\theta} \cos\theta \end{pmatrix} = \begin{pmatrix} \cos\theta & -\rho \sin\theta \\ \sin\theta & \rho \cos\theta \end{pmatrix} \begin{pmatrix} \dot{\rho} \\ \dot{\theta} \end{pmatrix} = \boldsymbol{J}_t(\rho, \theta) \begin{pmatrix} \dot{\rho} \\ \dot{\theta} \end{pmatrix},$$

with $\det \boldsymbol{J}_t = \rho$. Therefore,

$$\begin{pmatrix} \dot\rho \\ \dot\theta \end{pmatrix} = \boldsymbol{J}_t^{-1}(\rho,\theta)\begin{pmatrix} \dot u \\ \dot v \end{pmatrix} = \begin{pmatrix} \cos\theta & \sin\theta \\ -\dfrac{\sin\theta}{\rho} & \dfrac{\cos\theta}{\rho} \end{pmatrix}\begin{pmatrix} \dot u \\ \dot v \end{pmatrix}, \quad \text{provided that } \rho = \sqrt{u^2+v^2} \neq 0.$$

Evaluating then

$$\begin{aligned} \boldsymbol{J}_{p,t}(\rho,\theta,\lambda,Z) &= \boldsymbol{J}_p(u,v,\lambda,Z)\big|_{\substack{u=\rho\cos\theta \\ v=\rho\sin\theta}} \\ &= \begin{pmatrix} -\dfrac{\lambda}{Z} & 0 & \dfrac{\rho\cos\theta}{Z} & \dfrac{\rho^2\sin\theta\cos\theta}{\lambda} & -\left(\lambda+\dfrac{\rho^2\cos^2\theta}{\lambda}\right) & \rho\sin\theta \\ 0 & -\dfrac{\lambda}{Z} & \dfrac{\rho\sin\theta}{Z} & \lambda+\dfrac{\rho^2\sin^2\theta}{\lambda} & -\dfrac{\rho^2\sin\theta\cos\theta}{\lambda} & -\rho\cos\theta \end{pmatrix}, \end{aligned}$$

we obtain

$$\begin{pmatrix} \dot\rho \\ \dot\theta \end{pmatrix} = \boldsymbol{J}_t^{-1}(\rho,\theta)\boldsymbol{J}_{p,t}(\rho,\theta,\lambda,Z)\begin{pmatrix} \boldsymbol{V} \\ \boldsymbol{\Omega} \end{pmatrix} = \boldsymbol{J}_{p,polar}(\rho,\theta,\lambda,Z)\begin{pmatrix} \boldsymbol{V} \\ \boldsymbol{\Omega} \end{pmatrix},$$

with

$$\boldsymbol{J}_{p,polar}(\rho,\theta,\lambda,Z) = \begin{pmatrix} -\dfrac{\lambda\cos\theta}{Z} & -\dfrac{\lambda\sin\theta}{Z} & \dfrac{\rho}{Z} & \dfrac{(\lambda^2+\rho^2)\sin\theta}{\lambda} & -\dfrac{(\lambda^2+\rho^2)\cos\theta}{\lambda} & 0 \\ \dfrac{\lambda\sin\theta}{\rho Z} & -\dfrac{\lambda\cos\theta}{\rho Z} & 0 & \dfrac{\lambda\cos\theta}{\rho} & \dfrac{\lambda\sin\theta}{\rho} & -1 \end{pmatrix}.$$

Comparing now the structural zeros of $\boldsymbol{J}_p(u,v,\lambda,Z)$ and $\boldsymbol{J}_{p,polar}(\rho,\theta,\lambda,Z)$, we see that in the first case the effects of V_x and V_y respectively on $\dot u$ and $\dot v$ are decoupled, whereas in the second case the decoupled effects of V_z and Ω_z are respectively on $\dot\rho$ and $\dot\theta$.

Finally, when the 3D Cartesian point $\boldsymbol{P}$ is sufficiently close to the optical axis ($\rho \to 0$), matrix $\boldsymbol{J}_t$ becomes ill-conditioned, meaning that small motions of the Cartesian point may then lead to huge variations of the chosen polar parameters —in particular of θ— in the image plane. To recover a regular behavior close to and across $\rho = 0$, the inverse of $\boldsymbol{J}_t$ may be replaced, for instance, by a damped least squares matrix with damping factor $\sigma^2 > 0$,

$$\begin{aligned} \boldsymbol{J}_t^{DLS}(\rho,\theta) &= \boldsymbol{J}_t^T(\rho,\theta)\left(\sigma^2\boldsymbol{I}_{2\times2} + \boldsymbol{J}_t(\rho,\theta)\boldsymbol{J}_t^T(\rho,\theta)\right)^{-1} \\ &= \begin{pmatrix} \cos\theta & \sin\theta \\ -\rho\sin\theta & \rho\cos\theta \end{pmatrix}\begin{pmatrix} \sigma^2+\cos^2\theta+\rho^2\sin^2\theta & (1-\rho^2)\sin\theta\cos\theta \\ (1-\rho^2)\sin\theta\cos\theta & \sigma^2+\sin^2\theta+\rho^2\cos^2\theta \end{pmatrix}^{-1} \\ &= \begin{pmatrix} \dfrac{\cos\theta}{1+\sigma^2} & \dfrac{\sin\theta}{1+\sigma^2} \\ -\dfrac{\rho\sin\theta}{\rho^2+\sigma^2} & \dfrac{\rho\cos\theta}{\rho^2+\sigma^2} \end{pmatrix}, \end{aligned}$$

with $\det(\boldsymbol{J}_t^{DLS}) = \rho/[\rho^2+\sigma^2)(1+\sigma^2)] > 0$ for $\sigma^2 > 0$ (and equal to $1/\rho$ for $\sigma^2 = 0$).

Exercise 3

We compute first the gravitational potential energy $U_g(\boldsymbol{q}) = U_1 + U_2 + U_3$, with

$$U_1 = 0, \qquad U_2 = m_2 g_0 d_2 \sin q_2, \qquad U_3 = m_3 g_0 (q_3 + d_3)\sin q_2.$$

Therefore, the gravity vector and its (minimal) linear parametrization are given by

$$\boldsymbol{g}(\boldsymbol{q}) = \left(\frac{\partial U_g(\boldsymbol{q})}{\partial \boldsymbol{q}}\right)^T = \begin{pmatrix} 0 \\ g_0\,(m_2 d_2 + m_3(q_3+d_3))\cos q_2 \\ g_0 m_3 \sin q_2 \end{pmatrix}$$

$$= \begin{pmatrix} 0 & 0 \\ g_0\, q_3 \cos q_2 & g_0 \cos q_2 \\ g_0 \sin q_2 & 0 \end{pmatrix} \begin{pmatrix} m_3 \\ m_2 d_2 + m_3 d_3 \end{pmatrix} = \boldsymbol{Y_g}(\boldsymbol{q})\,\boldsymbol{a_g},$$

with $p_g = \dim(\boldsymbol{a_g}) = 2$. The dynamic model (4) can thus be rewritten as

$$\boldsymbol{Y_M}(\boldsymbol{q},\dot{\boldsymbol{q}},\ddot{\boldsymbol{q}})\,\boldsymbol{a_M} + \boldsymbol{Y_g}(\boldsymbol{q})\,\boldsymbol{a_g} = \begin{pmatrix} \boldsymbol{Y_M}(\boldsymbol{q},\dot{\boldsymbol{q}},\ddot{\boldsymbol{q}}) & \boldsymbol{Y_g}(\boldsymbol{q}) \end{pmatrix} \begin{pmatrix} \boldsymbol{a_M} \\ \boldsymbol{a_g} \end{pmatrix} = \boldsymbol{Y}(\boldsymbol{q},\dot{\boldsymbol{q}},\ddot{\boldsymbol{q}})\,\boldsymbol{a} = \boldsymbol{\tau}.$$

Note that the linear parametrization of the dynamic model by $\boldsymbol{a}$ may not be minimal, since there could be some overlapping between the coefficients in $\boldsymbol{a}_M$ and those defined in $\boldsymbol{a}_g$.

Assuming that the values of all dynamic coefficients $\boldsymbol{a}$ are unknown, the adaptive trajectory tracking control takes the usual form

$$\begin{aligned} \boldsymbol{\tau} &= \boldsymbol{Y}(\boldsymbol{q},\dot{\boldsymbol{q}},\dot{\boldsymbol{q}}_r,\ddot{\boldsymbol{q}}_r)\hat{\boldsymbol{a}} + \boldsymbol{K}_P(\boldsymbol{q}_d - \boldsymbol{q}) + \boldsymbol{K}_D(\dot{\boldsymbol{q}}_d - \dot{\boldsymbol{q}}), \qquad \boldsymbol{K}_P, \boldsymbol{K}_D > 0 \\ \dot{\hat{\boldsymbol{a}}} &= \boldsymbol{\Gamma}\boldsymbol{Y}^T(\boldsymbol{q},\dot{\boldsymbol{q}},\dot{\boldsymbol{q}}_r,\ddot{\boldsymbol{q}}_r)\,(\dot{\boldsymbol{q}}_r - \dot{\boldsymbol{q}}), \qquad \boldsymbol{\Gamma} > 0, \end{aligned} \tag{5}$$

where $\dot{\boldsymbol{q}}_r = \dot{\boldsymbol{q}}_d + \boldsymbol{\Lambda}(\boldsymbol{q}_d - \boldsymbol{q})$, $\boldsymbol{\Lambda} > 0$, and

$$\boldsymbol{Y}(\boldsymbol{q},\dot{\boldsymbol{q}},\dot{\boldsymbol{q}}_r,\ddot{\boldsymbol{q}}_r) = \begin{pmatrix} \boldsymbol{Y_M}(\boldsymbol{q},\dot{\boldsymbol{q}},\dot{\boldsymbol{q}}_r,\ddot{\boldsymbol{q}}_r) & \boldsymbol{Y_g}(\boldsymbol{q}) \end{pmatrix} \hat{\boldsymbol{a}} = \hat{\boldsymbol{M}}(\boldsymbol{q})\ddot{\boldsymbol{q}}_r + \hat{\boldsymbol{C}}(\boldsymbol{q},\dot{\boldsymbol{q}})\dot{\boldsymbol{q}}_r + \hat{\boldsymbol{g}}(\boldsymbol{q}).$$

The number of states of the adaptive controller (5), i.e., the number of its defining differential equations, is equal to the number of updating dynamic coefficients: $\dim(\hat{\boldsymbol{a}}) = p_M + p_g = p_M + 2$.

Assuming that the values of the dynamic coefficients $\boldsymbol{a_M}$ are already known, one can define an adaptive trajectory control with the same global tracking properties of (5), but with a reduced number of states equal to $p_g = 2$. In fact, it is natural to define this controller as

$$\begin{aligned} \boldsymbol{\tau} &= \boldsymbol{Y}_M(\boldsymbol{q},\dot{\boldsymbol{q}},\dot{\boldsymbol{q}}_r,\ddot{\boldsymbol{q}}_r)\boldsymbol{a_M} + \boldsymbol{Y_g}(\boldsymbol{q})\hat{\boldsymbol{a}}_{\boldsymbol{g}} + \boldsymbol{K}_P(\boldsymbol{q}_d - \boldsymbol{q}) + \boldsymbol{K}_D(\dot{\boldsymbol{q}}_d - \dot{\boldsymbol{q}}), \qquad \boldsymbol{K}_P, \boldsymbol{K}_D > 0 \\ \dot{\hat{\boldsymbol{a}}}_{\boldsymbol{g}} &= \boldsymbol{\Gamma_g}\boldsymbol{Y}_{\boldsymbol{g}}^T(\boldsymbol{q})\,(\dot{\boldsymbol{q}}_r - \dot{\boldsymbol{q}}), \qquad \boldsymbol{\Gamma_g} > 0, \end{aligned} \tag{6}$$

where $\dot{\boldsymbol{q}}_r = \dot{\boldsymbol{q}}_d + \boldsymbol{\Lambda}(\boldsymbol{q}_d - \boldsymbol{q})$, $\boldsymbol{\Lambda} > 0$, and $\boldsymbol{Y_g}(\boldsymbol{q})\hat{\boldsymbol{a}}_{\boldsymbol{g}} = \hat{\boldsymbol{g}}(\boldsymbol{q})$.

The proof of global asymptotic stability of the tracking error follows the same lines of the proof holding for (5). The 'trick' in (6) that leads to this sufficient result stands in preserving the passivity structure also in the known term: namely, adopting $\dot{\boldsymbol{q}}_r$ and $\ddot{\boldsymbol{q}}_r$ in the evaluation of $\boldsymbol{Y_M}$ (and *not* $\dot{\boldsymbol{q}}$ only (or $\dot{\boldsymbol{q}}_d$) and $\ddot{\boldsymbol{q}}_d$), as well as using the skew-symmetric property of a suitable factorization $\boldsymbol{c}(\boldsymbol{q},\dot{\boldsymbol{q}}) = \boldsymbol{C}(\boldsymbol{q},\dot{\boldsymbol{q}})\dot{\boldsymbol{q}}$ of the Coriolis and centrifugal terms. More in detail, take the Lyapunov candidate

$$V_g = \frac{1}{2}\boldsymbol{s}^T\boldsymbol{M}(\boldsymbol{q})\boldsymbol{s} + \boldsymbol{e}^T\boldsymbol{K}_P\boldsymbol{e} + \frac{1}{2}\tilde{\boldsymbol{a}}_{\boldsymbol{g}}^T\boldsymbol{\Gamma_g}\tilde{\boldsymbol{a}}_{\boldsymbol{g}} \geq 0,$$

with $\boldsymbol{s} = \dot{\boldsymbol{q}}_r - \dot{\boldsymbol{q}}$, $\boldsymbol{e} = \boldsymbol{q}_d - \boldsymbol{q}$, $\boldsymbol{R} > 0$, and $\tilde{\boldsymbol{a}}_{\boldsymbol{g}} = \boldsymbol{a_g} - \hat{\boldsymbol{a}}_{\boldsymbol{g}}$. Its time derivative is

$$\dot{V}_g = \frac{1}{2}\boldsymbol{s}^T\dot{\boldsymbol{M}}(\boldsymbol{q})\boldsymbol{s} + \boldsymbol{s}^T\boldsymbol{M}(\boldsymbol{q})\dot{\boldsymbol{s}} + 2\boldsymbol{e}^T\boldsymbol{K}_P\dot{\boldsymbol{e}} - \tilde{\boldsymbol{a}}_{\boldsymbol{g}}^T\boldsymbol{\Gamma_g}\dot{\hat{\boldsymbol{a}}}_{\boldsymbol{g}}.$$

The closed-loop system under (6) satisfies the differential equation

$$\boldsymbol{M}(\boldsymbol{q})\ddot{\boldsymbol{q}} + \boldsymbol{C}(\boldsymbol{q},\dot{\boldsymbol{q}})\dot{\boldsymbol{q}} + \boldsymbol{g}(\boldsymbol{q}) = \boldsymbol{M}(\boldsymbol{q})\ddot{\boldsymbol{q}}_r + \boldsymbol{C}(\boldsymbol{q},\dot{\boldsymbol{q}})\dot{\boldsymbol{q}}_r + \hat{\boldsymbol{g}}(\boldsymbol{q}) + \boldsymbol{K}_P\boldsymbol{e} + \boldsymbol{K}_D\dot{\boldsymbol{e}}$$

or

$$\boldsymbol{M}(\boldsymbol{q})\dot{\boldsymbol{s}} + \boldsymbol{C}(\boldsymbol{q},\dot{\boldsymbol{q}})\boldsymbol{s} = \tilde{\boldsymbol{g}}(\boldsymbol{q}) - \boldsymbol{K}_P\boldsymbol{e} - \boldsymbol{K}_D\dot{\boldsymbol{e}}, \tag{7}$$

with $\tilde{\boldsymbol{g}}(\boldsymbol{q}) = \boldsymbol{g}(\boldsymbol{q}) - \hat{\boldsymbol{g}}(\boldsymbol{q}) = \boldsymbol{Y_g}(\boldsymbol{q})\boldsymbol{a_g} - \boldsymbol{Y_g}(\boldsymbol{q})\hat{\boldsymbol{a}}_{\boldsymbol{g}} = \boldsymbol{Y_g}(\boldsymbol{q})\tilde{\boldsymbol{a}}_{\boldsymbol{g}}$. When evaluated along the trajectories of (7), $\dot{V}_g$ becomes

$$\begin{aligned}
\dot{V}_g &= \frac{1}{2}\boldsymbol{s}^T\left(\dot{\boldsymbol{M}}(\boldsymbol{q}) - 2\boldsymbol{C}(\boldsymbol{q},\dot{\boldsymbol{q}})\right)\boldsymbol{s} + \boldsymbol{s}^T\left(\tilde{\boldsymbol{g}}(\boldsymbol{q}) - \boldsymbol{K}_P\boldsymbol{e} - \boldsymbol{K}_D\dot{\boldsymbol{e}}\right) + 2\,\boldsymbol{e}^T\boldsymbol{K}_P\dot{\boldsymbol{e}} - \tilde{\boldsymbol{a}}_{\boldsymbol{g}}^T\boldsymbol{\Gamma}_{\boldsymbol{g}}\dot{\hat{\boldsymbol{a}}}_{\boldsymbol{g}} \\
&= \boldsymbol{s}^T\left(\boldsymbol{Y_g}(\boldsymbol{q})\tilde{\boldsymbol{a}}_{\boldsymbol{g}} - \boldsymbol{K}_P\boldsymbol{e} - \boldsymbol{K}_D\dot{\boldsymbol{e}}\right) + 2\,\boldsymbol{e}^T\boldsymbol{K}_P\dot{\boldsymbol{e}} - \tilde{\boldsymbol{a}}_{\boldsymbol{g}}^T\boldsymbol{Y}_{\boldsymbol{g}}^T(\boldsymbol{q})\boldsymbol{s} \\
&= -\left(\dot{\boldsymbol{e}} + \boldsymbol{\Lambda}\boldsymbol{e}\right)^T\left(\boldsymbol{K}_P\boldsymbol{e} + \boldsymbol{K}_D\dot{\boldsymbol{e}}\right) + 2\,\boldsymbol{e}^T\boldsymbol{K}_P\dot{\boldsymbol{e}} \\
&= -\left(\dot{\boldsymbol{e}} + \boldsymbol{K}_D^{-1}\boldsymbol{K}_P\boldsymbol{e}\right)^T\left(\boldsymbol{K}_P\boldsymbol{e} + \boldsymbol{K}_D\dot{\boldsymbol{e}}\right) + 2\,\boldsymbol{e}^T\boldsymbol{K}_P\dot{\boldsymbol{e}} = -\boldsymbol{e}^T\boldsymbol{K}_P\boldsymbol{K}_D^{-1}\boldsymbol{K}_P\boldsymbol{e} - \dot{\boldsymbol{e}}^T\boldsymbol{K}_D\dot{\boldsymbol{e}} \le 0,
\end{aligned}$$

where the skew-symmetry of $\dot{\boldsymbol{M}} - 2\boldsymbol{C}$, the updating law for $\hat{\boldsymbol{a}}_{\boldsymbol{g}}$ in (6), and $\boldsymbol{\Lambda} = \boldsymbol{\Lambda}^T = \boldsymbol{K}_D^{-1}\boldsymbol{K}_P > 0$ (with diagonal PD gains) have been used. The rest of the proof follows as in the general case, using Barbalat lemma and LaSalle theorem.

Exercise 4

With reference to Fig. 3, the task frame is placed at the contact point between the spherical tool and the surface. The $\boldsymbol{z}_t$-axis is *always* aligned with the downward normal to the surface, no matter if the surface is locally flat or curved. One of the two other axes, say $\boldsymbol{x}_t$, can be chosen to be aligned with the desired polishing direction on the metallic surface. Remember that, in the modeling phase, the tool-surface contact is assumed to be rigid and *frictionless*. Therefore, the spherical tool can also slide without rolling in contact. Moreover, being the contact point-wise, there cannot be any moment applied by the tool at the contact.

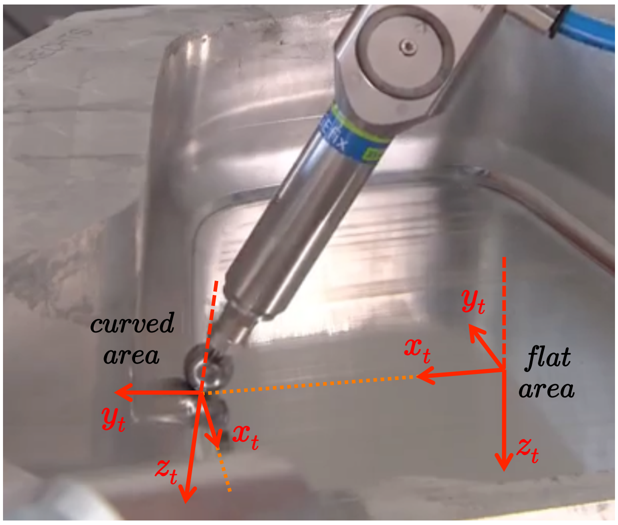

Figure 3: Task frame definition for the surface polishing of a metallic work piece.

According to the chosen task frame, the natural (geometric) constraints of this interaction problem are

$$v_z = 0, \quad F_x = 0, \quad F_y = 0, \quad M_x = 0, \quad M_y = 0, \quad M_z = 0,$$

while the artificial constraints are

$$F_z = F_{z,d} > 0, \quad v_x = v_{x,d} > 0, \quad v_y = v_{y,d} = 0, \quad \omega_x = \omega_{x,d}, \quad \omega_y = \omega_{y,d}, \quad \omega_z = \omega_{z,d}.$$

Therefore, a hybrid force-motion controller designed based on feedback linearization and decoupling will include five scalar position control loops and only one force control loop. The value $v_{y,d} = 0$ is related to the choice of the $\boldsymbol{x}_t$-axis being aligned with the tangent to the polishing path, which is executed at the speed $v_{x,d}$, that should be followed on the surface. Moreover, when there is no need to change the orientation of the tool (e.g., for avoiding collision with some lateral side of the work piece), we set $\boldsymbol{\omega}_d = \begin{pmatrix} \omega_{x,d} & \omega_{y,d} & \omega_{z,d} \end{pmatrix}^T = \mathbf{0}$. Finally, the positive value $F_{z,d}$ specifies the normal force needed for obtaining a satisfactory polishing result (by pressure).

* * * * *